Available online at www.sciencedirect.com
ScienceDirect
Tetrahedron: Asymmetry
Tetrahedron: *Asymmetry* 19 (2008) 97–110

Contributions to chromatographic chiral recognition of permethrinic acid stereoisomers by a quinine carbamate chiral selector: evidence from X-ray diffraction, DFT computations, ^{1}H NMR, and thermodynamic studies

Wolfgang Bicker,[a] Ion Chiorescu,[b] Vladimir B. Arion,[b] Michael Lämmerhofer[a,*] and Wolfgang Lindner[a]

[a]*Christian Doppler Laboratory for Molecular Recognition Materials, Department of Analytical Chemistry and Food Chemistry, University of Vienna, Waehringer Strasse 38, A-1090 Vienna, Austria*
[b]*Department of Inorganic Chemistry, University of Vienna, Waehringer Strasse 42, A-1090 Vienna, Austria*

Received 31 October 2007; accepted 30 November 2007

Abstract—A chiral stationary phase (CSP) based on *O*-9-(2,6-diisopropylphenylcarbamoyl)quinine (DIPPCQN) as a chiral selector (SO) exhibits remarkable stereoselectivity for the four stereoisomers of permethrinic acid, 3-(2,2-dichlorovinyl)-2,2-dimethylcyclopropanecarboxylic acid (DCCA), a precursor and prime metabolite of the pyrethroid-type insecticide permethrin. The four individual isomers of DCCA were crystallized as salts of DIPPCQN for crystal structure analysis to further our understanding of chiral recognition. X-ray diffraction structures revealed that the diastereomeric complexes displayed only minor differences in their geometries with regard to specific binding interactions. The common feature is an ionic hydrogen bond, which holds the SO-selectand (SO–SA) complexes together and fixes the individual ligands in the same single point in the binding pocket of the SO. Stereoselectivity seems to arise from distinct orientations of the cyclopropane ring and/or its substituents, which means that it is most likely the result of a plethora of weak non-covalent interactions (dispersion forces) or different steric environments for the substituents of the distinct guest stereoisomers. Herein, other interactive and discriminative forces are also discussed on the basis of the additivity of SO–SA binding contributions in accordance to a linear-free energy model for chiral distinction.
The chiral recognition mechanism as deduced from the diffraction data has been complemented by DFT computations, liquid chromatographic thermodynamic analysis, and ^{1}H NMR spectroscopy measurements. DFT computations (geometry optimization at the Hartree–Fock level and single point energy calculations at the B3LYP level) could correctly reproduce the relative binding strengths for the two enantiomers of *cis*- and *trans*-DCCA ($\Delta\Delta H$ −4.2 and −0.52 kJ mol^{-1}, respectively) and thus the chromatographic elution order of the enantiomers. Liquid chromatographic thermodynamic investigations are in reasonable agreement with the relative trends regarding enantiomer affinity and the difference in enthalpy changes upon complexation.
^{1}H NMR experiments in acetonitrile-D_3 confirmed that the *anti-open* conformation of the quinine carbamate SO is, like in the solid-state, the preferential binding conformation in solution phase as well. Other interactions than the ionic hydrogen bond could not be derived from ^{1}H NMR measurements and thus, in sharp contrast to X-ray diffraction, the ^{1}H NMR experiments undertaken did not allow to infer stereoselectivity contributions.

1. Introduction

Chiral recognition is a fundamental phenomenon when chiral molecular species interact with each other. However, there still exists a deficiency in the understanding of the underlying molecular basis and this holds for complex biological systems and small synthetic receptor-like systems, such as chiral chromatographic ligands as well.

For both, the so-called 'three-point attachment model' which states in its original form that a minimum of three configuration-dependent attractive contact points between

* Corresponding author. Tel.: +43 1 4277 52323; fax: +43 1 4277 9523; e-mail: michael.laemmerhofer@univie.ac.at

0957-4166/$ - see front matter © 2007 Elsevier Ltd. All rights reserved.
doi:10.1016/j.tetasy.2007.11.037

a chiral receptor and its complementary functional groups of a chiral substrate are required for chiral distinction is commonly invoked to explain the molecular phenomenon of chiral recognition.[1–4] Thereby, it is often overlooked or vagely stated that a fourth condition is necessary, namely that the substrate can approach the receptor only from the surface, but not from the interior.[5] Whatsoever, this 'three-point attachment model' has been frequently under debate.[3,5–7] It has been extended, as opposed to its original formulation in which only attractive interactions were considered, in the point that, for example, 'two interactions can be repulsive if the third one is strong enough to promote the formation of at least one of the two diastereomeric complexes'.[3] Models that utilized all four ligands of an asymmetric carbon ('four location model',[8] 'four-contact point model',[5] 'eight-center chiral recognition'[9]) as well as systems that needed less than three contact points[3,10] have been discussed in the literature.

Such mechanistic perceptions have been inferred from various experimental studies and theoretical considerations. However, X-ray diffraction has traditionally been a very popular means to study chiral recognition mechanisms of crystallized receptor–substrate complexes of both biological systems,[8,11,12] synthetic receptors,[13–17] and chromatographic selector (SO) moieties[18–28] as well. Such studies provide directly vivid images of how molecular species interact with each other in the solid-state. However, it is unfortunate, that in many instances, the structure of only one of the two or more diastereomeric complexes could be solved (while the other diastereomeric complexes often did not crystallize in associated form, and were destroyed in the X-ray beam or for some other reason are not currently available).[21,24–27] Hence, from such incomplete sets of X-ray structures, the differences in the diastereomeric complex geometries could not be elucidated, thus leaving open some room for speculation about the main source of chiral distinction.

Herein, we report X-ray crystal structures of four diastereomeric complexes composed of 3-(2,2-dichlorovinyl)-2,2-dimethylcyclopropane carboxylic acid (DCCA) (Fig. 1a), also known as permethrinic acid, and *O*-9-(2,6-diisopropylphenylcarbamoyl)quinine (DIPPCQN) (Fig. 1b) which is a valuable chromatographic chiral SO moiety if immobilized to chromatographic supports such as silica gel[29] (Fig. 1c).

This system was found to be rewarding for the investigation of chiral recognition for two main reasons: (i) DCCA is a precursor and a major metabolite of the pyrethroid-type pesticide permethrin and some other pyrethroid insecticides. These types of pesticides have received priorities in household usage and the US Environmental Protection Agency has raised some concerns on the chirality issues of these agrochemicals in the context of human exposure studies. Some inconsistencies were noticed in the literature regarding the absolute configuration assignment which can be clarified with the help of the present X-ray crystal structures.[30] (ii) This small acid poses a significant challenge for liquid-phase chiral recognition and liquid chromatographic enantiomer

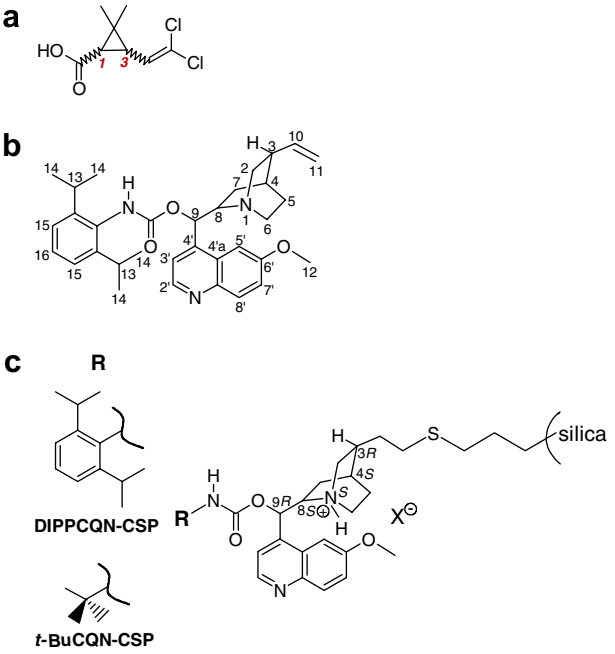

Figure 1. Structures of (a) DCCA selectand (SA), (b) the DIPPCQN selector (SO) along with atom numbering scheme employed for the ^{1}H NMR study, and (c) the corresponding quinine carbamate-based chiral stationary phases (CSPs) employed in the thermodynamic analyses.

separation but is a typical application for gas chromatographic enantiomer separation. The difficulty for chiral distinction arises from the fact that apart from the carboxylic acid functionality, additional supportive interaction sites such as extended aromatic groups or hydrogen donor–acceptor moieties are absent. However, permethrinic acid isomers can be stereoselectively recognized and chromatographically separated by quinine carbamate based chiral stationary phases (CSPs) (Fig. 1c) with enantioselectivity factors α for the *cis*- and *trans*-DCCA racemates up to 1.6 and 1.4, respectively (equivalent to $\Delta\Delta G \sim 1$ and 0.8 kJ mol^{-1}, respectively; for example, $k^{(1R,3R)\text{-}(+)\text{-}cis\text{-DCCA}} = 5.37$, $\alpha = 1.46$, elution order: (+) before (−); $k^{(1R,3S)\text{-}(+)\text{-}trans\text{-DCCA}} = 5.84$, $\alpha = 1.41$, elution order: (+) before (−) each on DIPPCQN-CSP with 0.25 % acetic acid in acetonitrile as eluent) which is quite remarkable considering the structural prerequisites of this small acid.[29]

The main goal of the present study was to gain insight into the stereodistinction mechanism of the DIPPCQN-SO for the DCCA selectand (SA) isomers. Due to the lack of clearly definable multiple interaction sites, it was unclear as to whether the present SO–SA system can be explained on the basis of the three-point interaction model. Such a three-point interaction is regarded to be imperative for effective chiral recognition. In this study, X-ray crystal structure analysis was complemented by supporting computational and ^{1}H NMR studies as well as thermodynamic investigations. In an attempt to depart from the three-point attachment model, chiral recognition contributions are discussed by an additivity model for stereoselectivity.

2. Results and discussion

2.1. X-ray crystal structures of *O*-9-(2,6-diisopropylphenylcarbamoyl)quininium 3-(2,2-dichlorovinyl)-2,2-dimethylcyclopropane carboxylates

Figures 2 and 3 show the X-ray diffraction structures for the individual stereoisomers of *cis*- and *trans*-DCCA.

It can be seen that the SO–SA complexes crystallize in a 1:1 molar ratio. The SO moiety of the complexes always adopts the energetically favorable '*anti-open*' conformation (vide infra) in which H8/H9 (atom numbering according to Fig. 1b) are in a *gauche* orientation and the quinuclidine nitrogen points away from the quinoline (*note*: in the '*closed*' conformation, in contrast, H8/H9 are in an *anti*-orientation and the quinuclidine nitrogen points toward the quinoline plane, which is located in front of the quinuclidine, obstructing easy access to the quinuclidinium ion-pairing and anion-exchange site, respectively).[24–27,31,32] The close approach of the nitrogen atom N2 of the SO and the carboxylate oxygen O4 of the SA (2.558(5), 2.563(2), 2.535(2), and 2.554(6) Å in **1**–**4**, respectively) (atom numbering according to Figs. 2 and 3) indicates the presence of a bonding interaction, which we can describe as an ionic hydrogen bond $N2^{+}$–H2···$^{-}$OOC.[33] Although this interaction between the charged centers is predominantly Coulombic in nature, it remains directional with $N2^{+}$–H2 pointing at O4 of the COO^{-} group. Such an interaction is well documented as salt-bridges between primary ammonium and carboxylate groups in biological systems.[34] The parameters of the hydrogen bonds are quoted in the legends to Figures 2 and 3. On the other hand, the values of interatomic distance N2···O5 of 3.244(5), 3.164(2), 3.172(2), and 3.209(7) Å, respectively, for **1**–**4** are clearly significantly larger. No other non-covalent bonds between the DCCA guest stereoisomers and the chiral quinine carbamate host can be derived from the X-ray crystal structures.

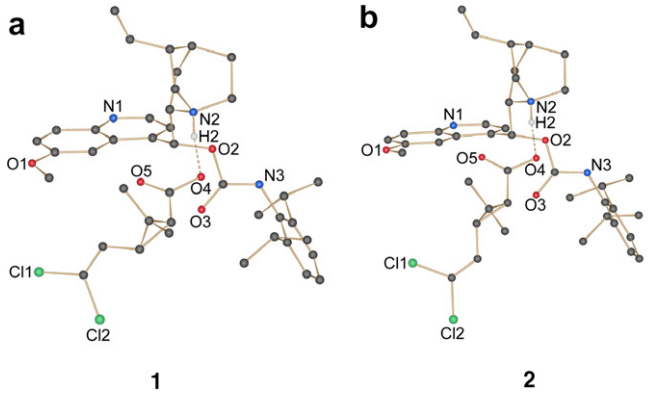

Figure 2. SCHAKAL view of the structures of (a) *O*-9-(2,6-diisopropylphenylcarbamoyl)quininium (1*R*,3*R*)-*cis*-DCCA **1** and (b) *O*-9-(2,6-diisopropylphenylcarbamoyl)quininium (1*R*,3*S*)-*trans*-DCCA **2**. Only components with larger site occupation factors in the disordered fragments are shown. All hydrogen atoms, except for H2 involved in the ionic hydrogen bonding, were omitted for clarity. Parameters of the ionic hydrogen bonding N2–H2···O4 (SO/SA) are as follows: (a) N2–H2 = 0.93, H2···O4 = 1.64, N2···O4 = 2.558(5) Å, ∠N2H2O4 = 170.9°; (b) N2–H2 = 0.93, H2···O4 = 1.64, N2···O4 = 2.563(2) Å, ∠N2H2O4 = 175.0°.

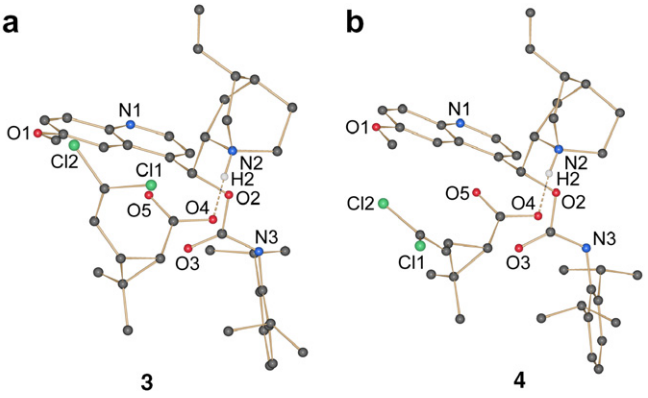

Figure 3. SCHAKAL view of the structures of (a) *O*-9-(2,6-diisopropylphenylcarbamoyl)quininium (1*S*,3*S*)-*cis*-DCCA **3** and (b) *O*-9-(2,6-diisopropylphenylcarbamoyl)quininium (1*S*,3*R*)-*trans*-DCCA **4**. All hydrogen atoms, except H2 involved in the ionic hydrogen bonding, were omitted for clarity. Parameters of the ionic hydrogen bonding N2–H2···O4 (SO/SA) are as follows: (a) N2–H2 = 0.93, H2···O4 = 1.61, N2···O4 = 2.535(2) Å, ∠N2H2O4 = 171.3°; (b) N2–H2 = 0.93, H2···O4 = 1.63, N2···O4 = 2.554(6) Å, ∠N2H2O4 = 171.2°.

With regard to the DCCA guest substructures in the complexes, the dichlorovinyl group and the carboxylate group lie on the same side of the plane spanned by the cyclopropane ring in compounds **1** and **3** and on opposite sides in compounds **2** and **4**, as expected for the *cis*- and *trans*-DCCA isomers, respectively. The resemblance of the carboxylate arrangement toward the quinuclidinium ring in all four diastereomeric complexes is remarkable and is made possible by the relative orientation of the cyclopropane ring with the two methyl groups pointing upwards in the two DCCA complexes with a (1*R*)-configuration (Fig. 2) and downwards in the two DCCA complexes with a (1*S*)-configuration (Fig. 3). By means of these X-ray data, the assignment of the absolute configurations of DCCA stereoisomers in earlier HPLC studies, which were based on linking the measured signs of specific rotation to literature data,[29] could now be unequivocally confirmed, that is (1*R*,3*R*)-(+)-*cis*-DCCA, (1*S*,3*S*)-(−)-*cis*-DCCA, (1*R*,3*S*)-(+)-*trans*-DCCA, (1*S*,3*R*)-(−)-*trans*-DCCA.[30]

2.2. Computational investigations

The density-functional theory (DFT) based computational model (for computational details see Section 4) was used to compute the differences in the binding energies $\Delta\Delta H$ of the complexation reactions between the chiral SO from the X-ray study, that is DIPPCQN, and the *cis*- as well as *trans*-DCCA enantiomers, as model for the chromatographic situation. Similar ab initio methods have already been employed for the geometry optimization of cinchona alkaloids[35] and complexes between cinchonan carbamates with amino acid derivatives.[36]

As is common for such computations quasi simulating a chromatographic system, a number of simplifying approximations were made.[37,38] The calculations have been

performed on the SO moiety which is the active site for chiral recognition. It should, however, be noted that under chromatographic conditions, interactions of the SAs with the support and/or achiral tether are not necessarily negligible in terms of enantiomer separation, even though these interactions occur non-stereoselectively. Yet, as so-called 'non-specific' interactions they may reduce the overall observed enantiodiscrimination level.[39] Thus, in our idealized view, the chiral distinction process of the present DIPPCQN-SO between opposite enantiomers of the chiral *cis*- and *trans*-DCCA SA can be described by two equilibria for each pair of enantiomers (Eqs. 1a and 1b) wherein 1(*S*)-enantiomers have a higher affinity toward the SO and thus are more strongly retained.

$$\begin{aligned}&\text{DIPPCQN} + (1R,3R)\text{-DCCA} \rightleftharpoons \text{DIPPCQN}\cdot(1R,3R)\text{-DCCA}\\&\text{DIPPCQN} + (1S,3S)\text{-DCCA} \rightleftharpoons \text{DIPPCQN}\cdot(1S,3S)\text{-DCCA}\end{aligned} \tag{1a}$$

and

$$\begin{aligned}&\text{DIPPCQN} + (1R,3S)\text{-DCCA} \rightleftharpoons \text{DIPPCQN}\cdot(1R,3S)\text{-DCCA}\\&\text{DIPPCQN} + (1S,3R)\text{-DCCA} \rightleftharpoons \text{DIPPCQN}\cdot 1S,3R)\text{-DCCA}\end{aligned} \tag{1b}$$

Via the differential free energies ($\Delta\Delta G$) of these equilibrium processes, it was possible to evaluate the level of enantiorecognition, because the free energy differences for the SO–SA complexes of the respective enantiomers are directly related to the α-value according to Eq. 2

$$\Delta\Delta G = \Delta G_S - \Delta G_R = -RT\ln\alpha \tag{2}$$

where α is a measure of the enantioselectivity of the SO in the chromatographic separation, which is experimentally readily available. In general, free energies ΔG are made up of enthalpic and entropic contributions as described by the Gibbs–Helmholtz equation. Its combination with Eq. 2 gives Eq. 3

$$\ln\alpha = -\frac{1}{T}\cdot\frac{\Delta\Delta H}{R} + \frac{\Delta\Delta S}{R} \tag{3}$$

The evaluation of the free energies of complexation is a complicated and time consuming procedure and therefore the difference in the enthalpy change upon complexation ($\Delta\Delta H$) has solely been calculated. Solvation effects and entropy differences have not been considered herein for the sake of simplicity. In earlier reports, for example, in the pioneering work on computational studies of the stereospecificity of chymotrypsin,[40] such contributions were assumed negligible, because they were supposed to cancel out if reactions are closely similar such as for stereoisomers. Although this is not completely true (vide infra), this approach was successfully used in several theoretical studies on the enantioselectivity of various CSPs.[37] The left side of the complexation processes in Eqs. 1a and 1b is energetically identical for enantiomers. Thus, the calculation of the free energies of the SO–SA complexes allows us to assess the relative complex stabilities and hence the enantiomer elution order. This was found to be accurate enough to predict the elution order of enantiomers.[38]

In addition, a single favorable binding state rather than averages over ensemble minima was determined.[24,26,38] This assumption seems to be justified because the experimental X-ray geometries are supposed to represent global, or close to global, optima and ^{1}H NMR revealed that these binding conformations are highly populated and predominant in solution as well (vide infra).

First, the minimized complex structures (Hartree–Fock level using a 6-31G(d,p) basis set) were compared with the X-ray geometries. The comparisons of the relevant calculated geometrical parameters with the experimentally obtained ones are given in Table 1.

The dihedral angle notations determining the *syn*/*anti* (T_1) and the *closed*/*open* (T_2) conformations are presented and are the same as in the work by Caner et al.[32] The distances between the quinuclidinic nitrogen atom and the carboxylic oxygen atom of DCCA are also quoted. The experimentally found *anti-open* conformations were preserved during the optimizations.

From the optimized complex geometries, the differential binding energies could be readily derived by single point DFT calculations [B3LYP[41] density-functional level using Duning's correlation consistent basis set of triple-zeta quality (cc-pvTZ) with corrections for basis set superposition

Table 1. Calculated and experimentally found geometrical parameters (T_1 = C4′a–C4′–C9–C8; T_2 = N1–C8–C9–C4′) (atom numbering according to Fig. 1b)

	(1*R*,3*R*)		(1*R*,3*S*)		(1*S*,3*S*)		(1*S*,3*R*)	
	Calcd	Exp.	Calcd	Exp.	Calcd	Exp.	Calcd	Exp.
T_1 (°)	−73	−73.9	−76.9	−74.8	−74.6	−78.3	−74.5	−73.9
T_2 (°)	−179	−174.8	−178.4	−176.2	−178.3	−171.9	−178.8	−178
N–O (Å)	2.5259	2.558(5)	2.5471	2.563(2)	2.5345	2.535(2)	2.5397	2.554(6)

Table 2. Calculated gas-phase differential binding energies ($\Delta\Delta H$) of the optimized SO–SA complex geometries as well as thermodynamic parameters for the HPLC enantiomer separations of *cis*- and *trans*-DCCA on cinchonan carbamate-type CSPs

Eluent[a]	*cis*-DCCA[c]					*trans*-DCCA[d]				
	$\Delta\Delta H$ [kJ mol^{-1}]	$\Delta\Delta S$ [J mol^{-1} K^{-1}]	$T\,\Delta\Delta S$[b] [kJ mol^{-1}]	% $T\,\Delta\Delta S$ (rel. to $\Delta\Delta H$)	$\Delta\Delta G$[b] [kJ mol^{-1}]	$\Delta\Delta H$ [kJ mol^{-1}]	$\Delta\Delta S$ [J mol^{-1} K^{-1}]	$T\,\Delta\Delta S$[b] [kJ mol^{-1}]	% $T\,\Delta\Delta S$ (rel. to $\Delta\Delta H$)	$\Delta\Delta G$[b] [kJ mol^{-1}]
DIPPCQN-CSP										
Gas-phase (computation)[g]	−4.20[e]					−0.52[f]				
MeOH	−1.78 (±0.07)	−4.19 (±0.25)	−1.25 (±0.07)	70	−0.53 (±0.10)	−1.50 (±0.07)	−3.28 (±0.02)	−0.98 (±0.01)	65	−0.53 (±0.02)
ACN	−2.30 (±0.08)	−4.44 (±0.26)	−1.32 (±0.08)	58	−0.98 (±0.11)	−1.25 (±0.05)	−1.45 (±0.17)	−0.43 (±0.05)	34	−0.82 (±0.06)
MeOH–water (80:20; v/v)	−2.94 (±0.31)	−8.08 (±1.03)	−2.41 (±0.31)	82	−0.54 (±0.43)	−1.50 (±0.08)	−3.65 (±0.27)	−1.09 (±0.08)	73	−0.41 (±0.08)
t-BuCQN-CSP										
MeOH	−1.48 (±0.05)	−3.26 (±0.15)	−0.97 (±0.05)	66	−0.51 (±0.07)	−1.31 (±0.05)	−2.81 (±0.17)	−0.84 (±0.05)	64	−0.47 (±0.06)
ACN	−1.44 (±0.14)	−3.13 (±0.47)	−0.93 (±0.14)	65	−0.51 (±0.20)	−1.05 (±0.13)	−1.12 (±0.45)	−0.34 (±0.13)	32	−0.71 (±0.16)
MeOH–water (80:20; *v/v*)	−2.09 (±0.07)	−5.35 (±0.22)	−1.60 (±0.07)	77	−0.49 (±0.09)	−1.20 (±0.03)	−2.86 (±0.11)	−0.85 (±0.03)	71	−0.34 (±0.04)

[a] Always containing 0.1% (v/v) acetic acid.
[b] Calculated for $T = 298$ K.
[c] (1*S*,3*S*)-*cis*-DCCA is more strongly retained; (1*R*,3*R*)-*cis*-DCCA is weakly retained.
[d] (1*S*,3*R*)-*trans*-DCCA is more strongly retained; (1*R*,3*S*)-*trans*-DCCA is weakly retained.
[e] The complex with (1*R*,3*R*)-configuration has less negative binding energy values (less exotherm) thus being less stable, while the complex with the (1*S*,3*S*)-configuration adopts a more negative binding energy (more exotherm) representing the more stable complex.
[f] The complex with the (1*R*,3*S*)-configuration is the one with less exotherm binding energies in the computations thus forming the weakly binding associate while the one with a (1*S*,3*R*)-configuration is the one with more exotherm binding energies and thus the stronger binding complex.
[g] Calculations performed with soluble CSP analogue, that is the DIPPCQN-selector.

errors using counterpoise[42] algorithm]. The $\Delta\Delta H$ values were calculated as the difference in energy of the optimized minima of the (1*S*,3*S*)- versus (1*R*,3*R*)-complexes (*cis*-complexes) as well as (1*S*,3*R*)- versus (1*R*,3*S*)-complexes (*trans*-complexes). The results are summarized in Table 2.

The relative binding strengths for the corresponding enantiomers ($\Delta\Delta H$ −4.2 and −0.52 kJ mol^{-1} for *cis*- and *trans*-complexes, respectively) and the enantiomer elution orders could be reproduced correctly by the computations. This may be regarded as an indication that the structural differences in the corresponding diastereomeric complexes, although at first glance very similar, are large enough to explain the chiral distinction process on the basis of the predominant binding conformations.

However, it should be noted that the DFT calculations do not adequately address all of the inter- and intramolecular interactions and solvation situations, which are probably of importance (vide infra) but are not taken into account explicitly. These arguments should be regarded as further caveats to avoid overinterpretations of the DFT structures because of these uncertainties.

2.3. Thermodynamics of adsorption and enantiomer separation

The thermodynamics of the adsorption and the enantiomer separation of *cis*- and *trans*-DCCA have been examined on a DIPPCQN-CSP in comparison to one of its structural analogs, the *O*-9-(*tert*-butylcarbamoyl)quinine (*t*-BuCQN) CSP (Fig. 1c) to obtain some information on the effect of the carbamate residue for the chiral recognition capability. Thereby, entropic contributions, which are not considered in the computations, may be detached from the differential free energies revealing the mere enthalpic contributions to the separations. These should be better comparable with the results from the computations, than the corresponding Gibbs free energy values that are often employed for the experimental verification of computational results. For this purpose, the separations of *cis*- and *trans*-DCCA have been performed at variable temperatures (10–40 °C) and the thermodynamic quantities have been derived according to Eq. 3 from the respective van't Hoff plots.[43,44] Although such thermodynamic measurements do not pursue the highest level of complexity and differentiation because they neglect the surface heterogeneity with its distinct adsorption sites,[39,45,46] they are supposed to be valuable for interpretations and the comparison with DFT calculations. The results are summarized in Table 2.

In any case, the adsorption of DCCA stereoisomers was enthalpically controlled under all eluent conditions investigated (exothermic adsorption processes with ΔH values between −14 and −21 kJ mol^{-1}). The adsorption enthalpies on the DIPPCQN-CSP were slightly less exothermic with methanol (MeOH) than with acetonitrile (ACN) and more exothermic with a MeOH–water (80:20; v/v) mixture [always containing 0.1% acetic acid (AcOH) as a source of counter-ion]. The increase in the heats of adsorption $-\Delta H$ with ACN may be explained by the strengthened ionic hydrogen-bond interaction, which can be readily competed by the protic MeOH solvent molecules (note that the dielectric shielding is supposed to be a little stronger in ACN than in MeOH). On the other hand, a further increase in the adsorption enthalpies with MeOH–water mixtures may be due to the fact that van der Waals type, that is dispersion, interactions may come into play. These solvent effects were slightly more pronounced for the *cis*-DCCA enantiomer pair than for the *trans*-pair and were negligible for the *t*-BuCQN-CSP (especially for the *trans*-pair). At this point it should be emphasized that in general, both stereoselective and non-stereoselective adsorption processes may contribute to these net adsorption enthalpies and they have not been deconvoluted.[39,45,46] However, the overall dominating role of the specific ionic hydrogen bond is quite clear which may, under linear chromatography conditions, render non-specific adsorption processes at other binding sites than the SO rather negligible.

From our perspective, the thermodynamic quantities of the enantiomer separations are of prime interest. These were generally dominated by enthalpic contributions ($\Delta\Delta H$ values between −1.05 and −2.94 kJ mol^{-1}) (Table 2). It can also be seen that the entropy term amounted to a considerable energy contribution (32–82% relative to the enthalpy term). Due to the same signs of $\Delta\Delta H$ and $\Delta\Delta S$, the latter exerts an opposite effect on the separation ('compensation effect'), that is, $\Delta\Delta G$ and separation factors become smaller in their magnitudes due to opposing entropic contributions. In other words, the enantiomer separations are worse than they could be without the entropic contributions.[44]

There are a few other noticeable details seen from Table 2. In case of *cis*-DCCA, the two distinct CSPs behave differently especially with regard to ACN as the solvent. While on the DIPPCQN-CSP, an increasing enthalpy difference $\Delta\Delta H$ is noticed when the solvent is exchanged from MeOH to ACN and MeOH–water, the compensation effect does not follow the same order. Hence, the favorable enantiodiscrimination capabilities of the DIPPCQN-CSP with the ACN-based eluent appear to be the combined effect of a gain in the differential adsorption enthalpies and a relatively lower entropic compensation effect $T \cdot \Delta\Delta S$ (58% related to $\Delta\Delta H$). As a result, the separation is about twice as good in terms of differential free energies $\Delta\Delta G$ with the ACN-based eluent than with the MeOH-based mobile phase. On the *t*-BuCQN-CSP the MeOH and ACN eluents produce quite similar $\Delta\Delta H$ and $\Delta\Delta S$ values for *cis*-DCCA. The MeOH–water eluent in contrast shows an increase in the magnitude of $-\Delta\Delta H$, yet this gain in differential enthalpy change is compensated for by the higher entropic cost $\Delta\Delta S$. The final outcome is that all eluents give approximately the same $\Delta\Delta G$ and separation factors, respectively.

For the *trans*-DCCA enantiomer separation, the investigated CSPs show the same trends. Again, the ACN eluent gives better separations (larger numerical values in terms of $-\Delta\Delta G$) despite a smaller $-\Delta\Delta H$ value because the compensation effect is substantially lower.

Overall, $\Delta\Delta H$ values from thermodynamic studies better reflect the relationship of the DFT computations than the $\Delta\Delta G$ values as calculated by Eq. 2 from the chromato-

graphic α-values, which are more frequently utilized for such purposes of comparison.[38] As mentioned above, the general trends have been correctly reproduced by the computations in agreement with the chromatographic experiments. Still, the calculations do overestimate the separation of the *cis*-enantiomer pair and underestimate that of the *trans*-enantiomer pair of DCCA. A part of the disagreement may be ascribed to the neglect of solvation in the DFT calculations and the assumption of a single global-minimum binding state rather than ensemble averages. Furthermore, the experimental chromatographic data reflect the sum of any adsorption processes, that is specific interactions with the SO and, if existent, any non-specific interactions at other sites of the CSP surface such as the achiral support/tether as well (they are supposed to reduce the $-\Delta\Delta H$ values to a certain extent). In general, however, it must be noted that the energy differences for the diastereomeric complexes are relatively small (<5 kJ mol^{-1}), which bears a higher risk of uncertainties in the computations.

2.4. ^{1}H NMR studies

To evaluate correlations between the solid-state geometries and the solution-phase binding geometries that are most likely closer to the situation under chromatographic conditions on the surface of the DIPPCQN-CSP, ^{1}H NMR investigations with free DIPPCQN-SO (as base and HCl salt), free *cis*- and *trans*-DCCA (in acidic form and as triethylammonium salts) as well as the corresponding SO–SA complexes have been carried out. The measurements were performed in ACN-D_3 (the solvent that gave the most promising separations under chromatographic conditions) as well as ACN-D_3 containing 0.25% D_3-AcOD (about twofold-molar excess in relation to the dissolved salt) which better matches the chromatographic eluent conditions.

The first question addressed was related to the preferential conformations[27,31,32,35] of the SO in free and bound states. This information can be deduced from the vicinal $^3J_{H8H9}$ coupling constants of the proton at the C9-carbon and from intramolecular NOEs between protons characteristic for a specific one of the three most abundant conformations of cinchona alkaloids and derivatives, respectively, viz. the *anti-open*, *anti-closed*, and *syn-closed* conformers (T_1 C4′a–C4′–C9–C8 refers to the *anti*/*syn*-orientation and is about −90° in *anti*-orientation and +90° in *syn*-orientation; T_2 N2–C8–C9–C4′ relates to *open*/*closed* conformational arrangement and adopts −180° in *open* and −60° in *closed* conformation[27,32]). Earlier investigations with homologs of the present SO such as *t*-BuCQN and *O*-9-(*tert*-butylcarbamoyl)-6′-neopentoxycinchonidine SOs, respectively, always rendered the cinchonan-SOs in a high population of the *anti-open* conformer, both in HCl–salt forms as well as when complexed with acidic guest molecules.[24,26,27] Bürgi and Baiker previously established a system to derive a quantitative measure of the populations of *open* and *closed* conformers of cinchona alkaloids from the vicinal $^3J_{H8H9}$ coupling constants by the application of a modified Kaplus equation.[35] Applied to the present host–guest systems, *open*/*closed* conformer ratios as outlined in Table 3 have been derived.

For the basic DIPPCQN-SO in its free form, an *open*/*closed* conformer ratio of about 30:70 percent can be found experimentally and this is in good agreement with the predictions on the basis of the dielectric constant of the medium (here: ACN $\varepsilon_r = 35.9$) making use of the system of Bürgi and Baiker established for cinchonidine.[35] As in the previous investigations, the HCl–salt of the SO predominantly exists in the *open*-conformation, while in the acetate salt there is still a noticeable percentage of *closed* conformer (ca. 40–50%) present. Likewise, in all the complexes of the DIPPCQN-SO with the DCCA stereoisomers, the same conformational tendency is found as for the acetate salt (see Table 3). This means that there is a considerable *closed–open* conformational transition upon complexation of the basic SO with the acidic DCCA isomers. However, it is consistently seen that the population of the *open*-conformation increases upon the addition of D_3-AcOD (from ca. 56% to ca. 71%). Such a behavior could be interpreted by a scenario in which the complex is in the ACN-D_3 solution partly dissociated into DCCA and DIPPCQN so that an averaged coupling constant of the free non-protonated SO (coexistence of *open* and *closed* conformations) and the fully protonated SO like in the HCl form (solely *open* conformation) is observed. When the solution of the complex is then acidified further by the addition of D_3-AcOD, a part of the DIPPCQN-SO of the dissociated complex gets protonated and undergoes the above mentioned *closed–open* conformational transition.

Table 3. Vicinal $^3J_{H8H9}$ coupling constants (Hz) of the diagnostic H9 proton and derived populations of *open* (P_{open}) and *closed* (P_{closed}) conformers[a]

Compound	Solvent	$^3J_{H8H9}$ (Hz)	P_{open}	P_{closed}
DIPPCQN (base)	ACN-D_3	7.20	0.30	0.70
DIPPCQN	ACN-D_3 + 0.25% D_3-AcOD	5.20	0.56	0.44
DIPPCQN·HCl	ACN-D_3	<2 (n.r.)	1.00	0.00
DIPPCQN·(1*S*,3*R*)-*trans*-DCCA	ACN-D_3	5.20	0.56	0.44
DIPPCQN·(1*S*,3*R*)-*trans*-DCCA	ACN-D_3 + 0.25% D_3-AcOD	4.00	0.71	0.29
DIPPCQN·(1*R*,3*S*)-*trans*-DCCA	ACN-D_3	5.20	0.56	0.44
DIPPCQN·(1*R*,3*S*)-*trans*-DCCA	ACN-D_3 + 0.25% D_3-AcOD	4.00	0.71	0.29
DIPPCQN·(1*S*,3*S*)-*cis*-DCCA	ACN-D_3	5.20	0.56	0.44
DIPPCQN·(1*S*,3*S*)-*cis*-DCCA	ACN-D_3 + 0.25% D_3-AcOD	4.00	0.71	0.29
DIPPCQN·(1*R*,3*R*)-*cis*-DCCA	ACN-D_3	5.20	0.56	0.44
DIPPCQN·(1*R*,3*R*)-*cis*-DCCA	ACN-D_3 + 0.25% D_3-AcOD	4.00	0.71	0.29

n.r. not resolved.

[a] Coupling constants of 1.7 and 9.6 Hz as suggested by Bürgi and Baiker[35] were taken as reference values for *open* and *closed* conformations, respectively.

Table 4. ^{1}H NMR chemical shifts (δ) of SO, SO as acetate and HCl salts, SAs, SAs as triethylammonium (TEA) salts, SO–SA complexes and complexation-induced shifts ($\Delta\delta$)

Proton[a]	δ[b] (ppm)	$\Delta\delta$[c,d] (ppm)		$\Delta\delta$[c,d] (ppm)				$\Delta\delta$[c,d] (ppm)				$\Delta\delta$[e] (ppm)			
	Free forms	Salt forms		*trans*-SA/SO complexes				*cis*-SA/SO complexes				$\Delta\delta$			
	Base/acid	AcOH salt of SO	HCl/TEA salts	(1*S*,3*R*)-Complex[f]		(1*R*,3*S*)-Complex[g]		(1*S*,3*S*)-Complex[h]		(1*R*,3*R*)-Complex[i]		(1*S*,3*R*)/(1*R*,3*S*)-Complex[e]		(1*S*,3*S*)/(1*R*,3*R*)-Complex[f]	
	(ACN-D_3)	(ACN-D_3)	(ACN-D_3)	(ACN-D_3)	(ACN-D_3 + 0.25% D_3-AcOD)	(ACN-D_3)	(ACN-D_3 + 0.25% D_3-AcOD)	(ACN-D_3)	(ACN-D_3 + 0.25% D_3-AcOD)	(ACN-D_3)	(ACN-D_3 + 0.25% D_3-AcOD)	(ACN-D_3)	(ACN-D_3 + 0.25% D_3-AcOD)	(ACN-D_3)	(ACN-D_3 + 0.25% D_3-AcOD)
DIPPCQN selector															
H2′	8.72	0.02	0.07	0.02	0.03	0.02	0.03	0.02	0.03	0.01	0.03	0.00	0.00	−0.01	0.00
H8′	7.97	0.01	0.12	0.00	0.01	0.01	0.01	0.00	0.02	0.00	0.02	0.01	0.00	0.00	0.00
H5′	7.55	−0.01	0.38	0.02	0.01	0.00	0.01	0.01	0.01	−0.01	0.00	−0.02	0.00	−0.02	−0.01
H3′	7.51	0.03	0.17	0.02	0.04	0.03	0.05	0.03	0.05	0.02	0.04	0.01	0.00	−0.01	−0.01
H7′	7.38	0.01	0.08	0.00	0.02	0.01	0.02	0.01	0.02	0.01	0.02	0.01	0.00	0.00	0.00
H16 (p)	7.25	0.00	0.04	0.00	0.01	0.01	0.01	0.00	0.01	−0.01	0.01	0.01	0.00	−0.01	0.00
H15 (m)	7.12	0.01	0.05	0.01	0.02	0.02	0.02	0.01	0.03	0.01	0.02	0.01	0.00	0.00	−0.01
H9	6.26	0.19	1.09	0.22	0.33	0.21	0.31	0.24	0.34	0.19	0.31	−0.01	−0.02	−0.05	−0.03
H10	5.95	−0.07	−0.20	−0.08	−0.12	−0.08	−0.12	−0.08	−0.11	−0.08	−0.11	0.00	0.00	0.00	0.00
H11	4.99	0.02	0.11	0.04	0.04	0.05	0.04	0.05	0.05	0.04	0.05	0.01	0.00	−0.01	0.00
H11	5.04	−0.07	−0.02	−0.07	−0.08	−0.07	−0.08	−0.07	−0.07	−0.08	−0.07	0.00	0.00	−0.01	0.00
H12 (–OCH_3)	3.93	0.04	0.20	0.04	0.05	0.04	0.05	0.04	0.06	0.03	0.05	0.00	0.00	−0.01	−0.01
H8	3.44	0.02	0.25	0.03	0.05	0.03	0.05	0.03	0.06	0.02	0.04	0.00	0.00	−0.01	−0.02
H6	3.19	0.11	0.50	0.12	0.20	0.15	0.22	0.12	0.21	0.12	0.21	0.03	0.02	0.00	0.00
H13	2.97	0.05	0.16	0.04	0.10	0.04	0.10	−0.07	0.09	0.03	0.09	0.00	0.00	0.10	0.00
H2	2.95	0.15	0.53	0.16	0.25	0.16	0.24	0.17	0.26	0.14	0.24	0.00	−0.01	−0.03	−0.02
H6	2.58	0.19	0.67	0.22	0.31	0.23	0.30	0.21	0.31	0.19	0.29	0.01	−0.01	−0.02	−0.02
H2	2.58	0.11	0.50	0.14	0.18	0.12	0.18	0.11	0.18	0.09	0.18	−0.02	0.00	−0.02	0.00
H3	2.29	0.12	0.49	0.12	0.19	0.13	0.19	0.13	0.20	0.12	0.19	0.01	0.00	−0.01	−0.01
H7	1.96	−0.07	0.33	−0.08	−0.03	−0.03	0.00	−0.03	0.02	−0.06	0.00	0.05	0.03	−0.03	−0.02
H4	1.84	0.00	0.30	−0.02	−0.11	−0.01	−0.11	−0.02	−0.10	−0.01	−0.10	0.01	0.00	0.00	0.00
H5	1.79	0.10	0.54	0.13	0.14	0.12	0.17	0.11	0.15	0.11	0.14	−0.01	0.03	0.00	−0.01
H7	1.69	0.13	0.31	0.21	0.04	0.14	0.04	0.12	0.05	0.14	0.05	−0.07	0.00	0.02	0.00
H5	1.55	0.11	0.17	0.10	0.12	0.12	0.18	0.12	0.19	0.11	0.19	0.02	0.06	−0.01	0.00
H14	1.09	0.03	0.11	0.03	0.05	0.04	0.05	0.04	0.05	0.03	0.05	0.01	0.00	−0.01	0.00
trans-DCCA															
=CH	5.81		−0.02	−0.02	−0.02	−0.01	−0.02					0.01	0.00		
C3H	2.08		−0.04	−0.01	0.00	−0.01	−0.01					0.00	−0.01		
C1H	1.67		−0.04	−0.03	−0.02	−0.03	−0.02					0.00	0.00		
Me1	1.23		0.00	0.00	0.00	0.00	0.00					0.00	0.00		
Me2	1.17		−0.03	−0.02	−0.02	−0.02	−0.02					0.00	0.00		
cis-DCCA															
=CH	6.27		0.13					0.13	0.11	0.11	0.09			−0.02	−0.02
C3H	2.03		−0.12					−0.09	−0.07	−0.10	−0.07			−0.01	0.00
C1H	1.85		−0.04					−0.04	−0.02	−0.04	−0.03			0.00	−0.01
Me1	1.22		−0.01					−0.02	−0.01	−0.03	−0.02			−0.01	−0.01
Me2	1.21		−0.02					−0.02	−0.01	−0.02	−0.01			0.00	0.00

[a] For numbering of protons see Figure 1a and b.

[b] Chemical shifts referred to internal tetramethyl silane.

[c] Salt-formation and complexation-induced shifts are reported relative to the free non-ionized forms.

[d] Negative sign denotes an upfield shift; positive sign a downfield shift.

[e] Chemical shift differences between complexes of corresponding enantiomers.

[f] DIPPCQN·(1*S*,3*R*)-*trans*-DCCA (strong complex).

[g] DIPPCQN·(1*R*,3*S*)-*trans*-DCCA (weak complex).

[h] DIPPCQN·(1*S*,3*S*)-*cis*-DCCA (strong complex).

[i] DIPPCQN·(1*R*,3*R*)-*cis*-DCCA (weak complex).

The discussed conformational preferences are also supported by the existence of characteristic intramolecular NOEs in the 2D-NOESY spectra. For example, the interring NOE between H3′ (quinoline) and H7 (quinuclidine) is indicative for the *anti-open* conformation and was detected in all the spectra of the DIPPCQN salts and the complexes. On the other hand, the intramolecular NOEs between H5′–H6 and H3′–H6 are characteristic for the presence of *anti-closed* and *syn-closed* conformers and could be readily found in the spectrum of the DIPPCQN base. Overall, the ^{1}H NMR spectra suggest that the situation regarding the conformational arrangements of the SO in solution is slightly more diverse than in the solid-state and besides the preferential *open*-conformation other conformers may exist, maybe due to dissociated complex. However under chromatographic conditions, the *anti-open* conformation of the SO, which allows the close approach of the acidic guest molecules toward the quinuclidine ion-exchange site, appears to be at least about 70%, which is still the most populated conformation. Stereoselective differences of the conformational behavior in the various complexes, by contrast, are not at all evident from the ^{1}H NMR spectra.

^{1}H NMR may also be an appropriate tool for obtaining information on the occurrence of intermolecular interactions in host–guest complexes. Upon complexation, SO–SA interactions may cause changes in the electronic microenvironment leading to the shielding or deshielding of specific protons that are involved in the intermolecular contacts which may be reflected as either downfield or upfield shifts in the proton NMR spectra relative to the free non-complexed molecular species. In this way, the existence and/or absence of (stereoselective) π–π-interactions in complexes between cinchonan carbamates and aromatic guest molecules could be proven in the previous investigations.[24,26,27] In the present case it was of particular interest whether the dichlorovinyl group was capable of binding to the quinoline ring and/or to the 2,6-diisopropylphenyl moiety in a kind of π–π-interaction (aromatic stacking).

Table 4 shows the ^{1}H NMR chemical shifts of the protons in the DIPPCQN-SO, as well as DCCA, along with their upfield or downfield shifts upon salt formation and complexation, respectively.

Consistent with earlier findings,[24,26,27] most of the quinuclidine ring protons are shifted upon salt formation, most notably the protons H2 and H6 that are adjacent to the quinuclidine nitrogen which is selectively protonated upon salt formation and exerts an electron-withdrawing influence on the neighboring protons. This effect is more strongly in the HCl salt than in the acetate salt, which may indicate that in ACN the degree of salt formation is incomplete with the weak AcOH. The substantial shifts in the proton at the C9-carbon may be explained to a certain extent by the *closed–open* conformational transition in the course of the salt formation, which brings this proton into the influence of the deshielding part of the quinoline ring current.[24] Essentially the same shifts, both qualitatively and quantitatively, as in the spectra of the acetate salt, are observed when the DIPPCQN-SO is complexed with either enantiomer of *cis*- and *trans*-DCCA (Table 4).

This means that all stereoisomers of DCCA undergo ion-pair formation to a similar extent. It is, however, remarkable that upon the addition of D_3-AcOD to the complexes (^{1}H NMR measurements of the complexes in ACN-D_3 containing 0.25% D_3-AcOD) even larger shifts of the same protons can be observed. This is again an indication that the degree of complexation of DIPPCQN with the DCCA stereoisomers in ACN-D_3 solution is incomplete and that there is an equilibrium of complexed and uncomplexed DIPPCQN-SO. By the addition of D_3-AcOD, the uncomplexed (basic) SO becomes protonated, which causes an increase in the observed shifts and the above mentioned increase in the population of *open*-conformer. It should be noted that neither the quinoline proton signals nor the diisopropylphenyl proton signals display significant shifts upon complexation with DCCA in neither one of the diastereomeric complexes. Significant shifts were found for the vinyl proton and the proton at the C3-carbon of DCCA in the *cis*-complexes only. However, qualitatively and quantitatively, the same shifts are observed in the triethylammonium salt of DCCA meaning that these shifts cannot be ascribed to specific intermolecular interactions with the DIPPCQN-SO. Hence, it seems safe to assume that intermolecular π–π-interaction or aromatic stacking does not take place. Since all the shift differences between the (1*S*,3*R*)- and (1*R*,3*S*)-complexes (*trans*-complexes) as well as (1*S*,3*S*)- and (1*R*,3*R*)-complexes (*cis*-complexes) are not significant (<0.1 ppm) it must be concluded that no stereoselective effects that could be ascribed to strong non-covalent intermolecular interactions are evident from the current set of ^{1}H NMR data.

In conclusion, it is postulated that the *anti-open* conformation is the preferential binding conformation as in solid-state while the occurrence of other conformational states may be ascribed to free SO originating from dissociated complex. Moreover, the ionic hydrogen bond, which holds the complex together, is the only intermolecular interaction that can be clearly derived from ^{1}H NMR and this occurs non-stereoselectively, that is largely to the same extent in the four complexes. Intermolecular π–π-interactions are not found nor any other supportive strong non-covalent (stereoselective) interactions. Moreover, no intermolecular NOEs that would indicate close intermolecular contacts could be identified in the complexes. Thus, the stereorecognition capability of the DIPPCQN SO for DCCA isomers cannot be rationalized on the basis of the ^{1}H NMR measurements undertaken.

2.5. Discussion of the chiral recognition mechanism

From the above discussed experimental results of the X-ray crystal structure analysis, the DFT computations, and the ^{1}H NMR spectroscopic investigations, it became evident that strong non-covalent bonds between the SO and the DCCA stereoisomers are restricted to the ionic hydrogen bonds that are supposedly the driving force for ion-pair formation and occur at the first glance non-stereoselectively.

Spatial and structural similarities of the diastereomeric complexes (Fig. 4) are observed with closely matching DIPPCQN-SO conformations in the different solid-state structures and very similar ionic hydrogen bond geometry, in particular interatomic distances and angles (Table 1). However, small structural complex dissimilarities may be transformed into chromatographic enantioselectivities large enough to enable baseline separation by HPLC. Since it is not a distinct number or type of strong docking interaction forces (such as ionic interactions, hydrogen bonds or π–π-interactions in the diastereomeric complexes, which could result in a considerable difference of free energies of interaction $\Delta\Delta G_{int}$ it raises the question as to what else makes the DIPPCQN-based CSP capable of distinguishing between the enantiomers of *cis*- and *trans*-DCCA.

In general, in the absence of cooperative effects, host–guest binding may be in accordance to the LFER (linear-free energy relationship) formalism described by a number of additive contributions[47,48] as given by Eq. 4

$$\Delta G_{binding}^{SO\text{–}SA} = \Delta G_{solv} + \Delta G_{int} + \Delta G_{conf} + \Delta G_{motion} \quad (4)$$

wherein the individual terms account for the change in free energies upon SO–SA binding due to (1) solvation, (2) SO–SA interactions, (3) conformational changes in the SO and SA upon binding, (4) motional restrictions and residual motions in the complex. The latter term contains free energy contributions due to the loss of internal rotations in SO and SA, due to the loss of rotational and translational degrees of freedom, and due to new vibrational modes in associated state (Eq. 5)

$$\Delta G_{motion} = \Delta G_{rot} + \Delta G_{r/t} + \Delta G_{vib} \quad (5)$$

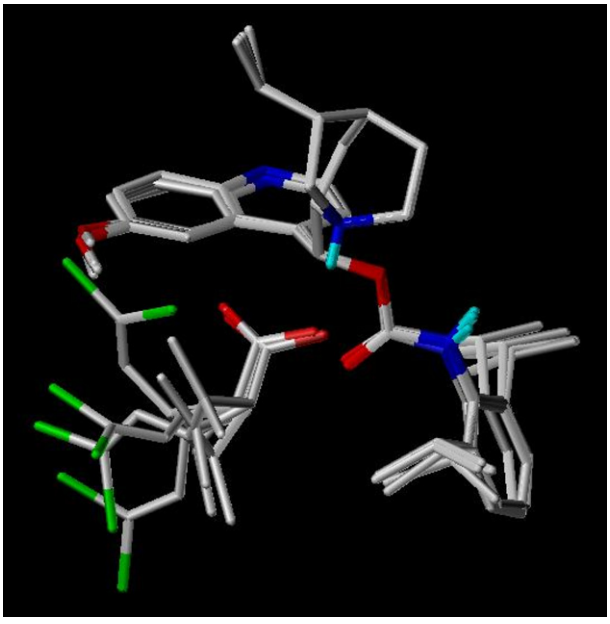

Figure 4. An overlay of single crystal X-ray structures of the four DIPPCQN–DCCA complexes (superposition by fit of quinuclidine and C9 carbon atoms) (structures have been processed with SYBYL LINUX version 7.0; most hydrogens have been omitted for clarity reasons).

Likewise, the chiral recognition process can be partitioned into several additive increments. Thus, even if the interaction term is identical for enantiomers (i.e., $\Delta\Delta G_{int} = 0$) there are supposed to be other components that might lead to chiral distinction. For example, in the course of complexation solvated functional groups must strip off the solvation shell before they can interact with appropriate (complementary) functional groups of the binding partners. This free energy contribution arising from desolvation is identical for the two diastereomeric complexes stemming from a specific SA racemate. After the formation of the non-covalent SO–SA binding interactions, the diastereomeric complexes are resolvated. This resolvation process may be different from an energetic view for diastereomeric complexes and may contribute to chiral distinction, that is $\Delta\Delta G_{solv} \neq 0$. The free energy component ΔG_{motion} is mostly entropic in nature. While the loss of translational and rotational degrees of freedom is supposed to be largely identical for two enantiomers, that is $\Delta\Delta G_{t/r} = 0$, both ΔG_{rot} and ΔG_{vib} are believed to be distinct in diastereomeric complexes. For example, if a rotatable group is exposed to the exterior in one of the diastereomeric complexes, it may retain its rotational degree of freedom. If such a rotation is sterically hindered and thus frozen in the other diastereomeric complex, a significant free energy difference $\Delta\Delta G_{rot} \neq 0$ may arise. The similar situation may be valid for the ΔG_{vib} component. Upon complexation, new vibrational modes are introduced and a looser complex may have a larger vibrational entropy contribution than a tighter one. Hence, such components might also contribute to chiral distinction.

Applied to the present case of diastereomeric complexes between DIPPCQN-SO with *cis*- and *trans*-DCCA enantiomers, chiral recognition is most likely a result of weak van der Waals or steric interactions (i.e., through a balance of repulsive steric collisions and/or attractive dispersive interactions). Such weak contributions in their sum seem to be discriminative enough because the DCCA stereoisomers are strongly bound to the SO via the directed ionic H-bond in the center of the binding pocket. The ligands are strongly fixed in the same single point in the binding pocket of the SO, and stereoselectivity seems to arise from distinct orientations of the cyclopropane ring and/or its substituents, that is upside down alignment in the complexes of the opposite enantiomers which holds for the *cis*- (Fig. 5a) as well as the *trans*-complexes (Fig. 5b).

Moreover, the guest molecules may, perhaps to a different extent, still have some residual motion in the binding cavity and the single flexible dichlorovinyl group may acquire different conformational spaces in the various diastereomeric complexes due to the distinct proximities of SO moieties. Further contributions may arise from solvent effects (in particular differences in the solvation, i.e., the resolvation of the complexes) as indicated by significant differences of the thermodynamic quantities for the distinct solvents (Table 2).

While the 'three-point attachment' model, in its original formulation appears at first glance to be less useful for explaining the chiral recognition of the presently investi-

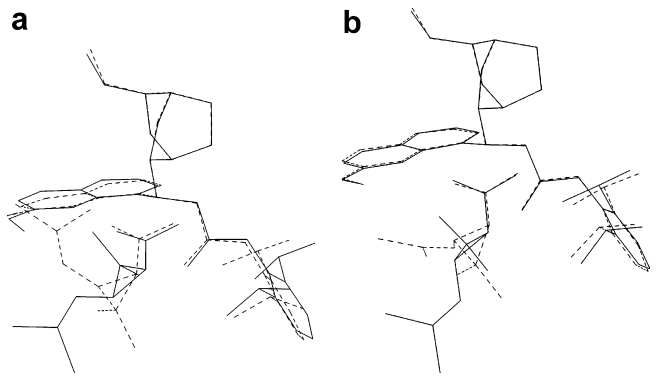

Figure 5. An overlay of X-ray structures of (a) *cis*-complexes **1** and **3** (solid lines: complex **1**; dashed lines: complex **3**), and (b) the *trans*-complexes **2** and **4** (solid lines: complex **2**; dashed lines: complex **4**).

gated SO–SA system, the later formulated more refined 'three-point interaction' model,[3] which considers any three dimensional interactions of whatever kind including strong and weak directed or non-directed binding interactions, steric repulsions, or non-isochronous solvation (i.e., directed interactions with solvent molecules), can be readily invoked to explain chiral recognition for the present molecular system.

DCCA can be considered as a particular molecule intrinsically containing one of the needed requirements, namely two of the four bonds of the asymmetric centers, which are incorporated into a rigid cyclopropane ring, are blocked which enforces a molecular rigidity and thus the stereoisomers are easier recognizable. It is a common perception that a single interaction with a rigid plane like the cyclopropane ring or its surface can count for at least two interaction sites. Hence the three-point interaction model seems to be obeyed also in the present molecular system. The molecular rigidity counts as one interaction site, the ionic hydrogen bond driven docking as the second and the possible van der Waals, steric, or polar chlorine interactions being the third one. Other contributions such as the free energy differences due to the differential resolvation of diastereomeric complexes or distinct motional behavior of complexed solute enantiomers may also help in the chiral recognition process of the DCCA stereoisomers by quinine carbamate receptors.

3. Conclusions

The availability of a full set of X-ray crystal structures of diastereomeric complexes of DCCA and DIPPCQN has opened up the avenue of obtaining detailed insight into favorable binding modes and chiral recognition mechanisms of this important acidic precursor of the pyrethroid pesticide permethrin by the cinchona alkaloid-type chromatographic SO moiety. These studies were further supported by ^{1}H NMR and computational studies, as well as chromatographic thermodynamic investigations. They revealed that the chromatographic enantiomer separations were dominated by enthalpic contributions and the favorable separation selectivity of ACN is largely due to a relatively lower entropic compensation effect. The DFT computations, which have to be interpreted with care, allowed us to reproduce the relative binding affinities and thus the enantiomer elution order.

^{1}H NMR confirmed that the *anti-open* conformation of the SO, which gives free access of the acidic guest molecules to the quinuclidine ion-exchange site and was found in the X-ray structures of all four diastereomeric complexes, appears to be, if not the exclusive, at least the highest populated binding conformation. In addition, ^{1}H NMR spectra revealed the existence of ion-pair formation (through an ionic hydrogen bond) in all four diastereomeric complexes as the primary interaction force that holds the complexes together. Other intermolecular interactions could not be found. The most obvious differences in the diastereomeric complexes of *cis*- and *trans*-DCCA with DIPPCQN, inferred from the solid-state X-ray diffraction structures, were found to be the different relative orientations of the methyl substituents at C2 and the dichlorovinyl at C3 of the cyclopropane ring within the binding pocket, which may result in weak discriminative forces such as steric collisions and/or dispersive interactions that may occur stereoselectively in these regions of the host–guest complexes and can be seen as the reason for the noteworthy enantiomer separations of DCCA on the quinine carbamate CSPs. Some other potential contributions to the chromatographic separation have also been discussed such as the differences in solvent effects, conformational spaces of substituents such as the dichlorovinyl group, and residual motions (dynamic flexibility of the guest in the complexes).

4. Experimental

4.1. Chemicals

Technical grade (1*RS*,3*RS*)-3-(2,2-dichlorovinyl)-2,2-dimethylcyclopropanecarboxylic acid (DCCA), consisting of about 40% *rac.-cis*-DCCA and about 60% *rac.-trans*-DCCA, was a gift from Agro-Chemie (Budapest, Hungary). The individual stereoisomers of DCCA were obtained by two-step preparative HPLC using first a RP18 column and then a Chiralpak QD-AX column as described elsewhere.[29,30] *O*-9-(2,6-Diisopropylphenylcarbamoyl)quinine (DIPPCQN) was prepared as reported elsewhere.[49] Acetic acid (AcOH), chloroform, dichloromethane, triethyl-amine (TEA) (all Fluka, Buchs, Switzerland), *n*-heptane (Fisher Scientific, Loughborough, UK), hydrochloric acid (HCl) (Merck, Darmstadt, Germany) were of analytical grade, acetonitrile (ACN) and methanol (MeOH) (both Fisher Scientific) of HPLC grade. Bidistilled water was used throughout.

4.2. Instrumentation

HPLC runs were carried out on an 1100 series liquid chromatography instrument from Agilent (Waldbronn, Germany) equipped with a diode array detector. ^{1}H NMR spectra were acquired on a Bruker DRX spectrometer with an operating frequency of 400 MHz (Bruker Optics, Vienna, Austria). X-ray analysis was performed with a

X8APEXII CCD diffractometer from Bruker AXS (Karlsruhe, Germany). The signs of the optical rotation were determined with a polarimeter model 341 from Perkin Elmer (Vienna, Austria).

4.3. Thermodynamic analysis

Studies of the thermodynamic parameters of the adsorption process of the DCCA stereoisomers on the stereoselective chiral stationary phases (CSPs) based on DIPPCQN and *O*-9-(*tert*-butylcarbamoyl)quinine (*t*-BuCQN) were carried out at a flow rate of 1 mL min^{-1} with 150 × 4.6 mm ID columns, thermostated by submerging them into the heating/cooling bath of a Haake F cryostat (model F6-C40, Haake, Karlsruhe, Germany). The eluent was pre-thermostated to the respective temperature by a Peltier cooling/heating element (column compartment of the Agilent 1100 series instrument) before it entered the column. The thermodynamic parameters were derived from the slopes and intercepts of Van't Hoff plots by linear regression analysis.

4.4. Crystal structure determination

The absolute configurations of the individual *cis*- and *trans*-DCCA stereoisomers were determined by X-ray analysis of the single co-crystals of (+)-*cis*-DCCA, (+)-*trans*-DCCA, (−)-*cis*-DCCA, and (−)-*trans*-DCCA, respectively, with DIPPCQN, which were grown from chloroform/*n*-heptane. *Note*: Signs of optical rotation of DCCA stereoisomers were determined in dichloromethane (*c* 1.5, $\lambda = 589$ nm, $T = 20$ °C)[30] and were in accordance with those reported previously by us.[29]

X-ray diffraction measurements were performed with graphite-monochromated Mo Kα radiation, $\lambda = 0.71073$ Å at 100(2) K. Single crystals were positioned at 40 mm from the detector and 1065, 4199, 5392, and 2936 frames were measured, each for 50, 30, 10, and 40 s over 1° scan width for complexes **1**, **2**, **3**, and **4** (vide infra), respectively. The data were processed using Bruker's software package.[50] The structures were solved by direct methods and refined by full-matrix least-squares techniques. Non-hydrogen atoms were refined with anisotropic displacement parameters (with the exception of the disordered fragment in compound **1**). Hydrogen atoms were placed in geometrically calculated positions and refined as riding atoms in the subsequent least squares model refinements. The isotropic thermal parameters were estimated to be 1.2 times the values of the equivalent isotropic thermal parameters of the atoms to which hydrogens were bonded. In compound **1** the dichlorovinyl fragment occupies two positions with different site occupation factors (SOF) 0.77 and 0.23. In compound **2** one methyl group of the isopropyl fragment was found to be disordered over two positions with different probability (SOF 0.64 for C32 and 0.36 for C32A). In the crystal structure of **4**, large voids have been observed which were marginally populated by *n*-heptane. For structure solution SHELXS-97,[51] for refinement SHELXL-97,[52] and for molecular diagrams SCHAKAL99[53] was used. Scattering factors were taken from the literature.[54] Details of the crystal data, data collection and refinement are as follows.[55]

4.4.1. *O*-9-(2,6-Diisopropylphenylcarbamoyl)quininium (1*R*, 3*R*)-(+)-*cis*-3-(2,2-dichlorovinyl)-2,2-dimethylcyclopropanecarboxylate 1. $C_{42}H_{52}Cl_5N_3O_5$, $M_r = 856.12$, monoclinic, space group $P2_1$ (no. 4), $a = 9.3667(3)$, $b = 15.0051(5)$, $c = 16.0350(5)$ Å, $\beta = 97.503(2)°$, $V = 2234.40(12)$ $Å^3$, $Z = 2$, $\rho_{calcd} = 1.272$ g cm^{-3}, $\mu = 0.369$ mm^{-1}. Of 32,478 reflections collected up to $\theta_{max} = 25°$, 7597 were independent, $R_{int} = 0.053$, and 5538 were observed ($I > 2\sigma(I)$); final *R* indices: $R_1 = 0.0642$, $wR_2 = 0.1700$ (all data); Flack parameter 0.01(9).

4.4.2. *O*-9-(2,6-Diisopropylphenylcarbamoyl)quininium (1*R*, 3*S*)-(+)-*trans*-3-(2,2-dichlorovinyl)-2,2-dimethylcyclopropanecarboxylate 2. $C_{42}H_{52}Cl_5N_3O_5$, $M_r = 856.12$, monoclinic, space group $P2_1$ (no. 4), $a = 9.3320(6)$, $b = 14.9915(10)$, $c = 16.0332(11)$ Å, $\beta = 93.853(2)°$, $V = 2238.0(3)$ $Å^3$, $Z = 2$, $\rho_{calcd} = 1.270$ g cm^{-3}, $\mu = 0.369$ mm^{-1}. Of 151,761 reflections collected up to $\theta_{max} = 27°$, 10,036 were independent, $R_{int} = 0.0655$, and 8360 were observed ($I > 2\sigma(I)$); final *R* indices: $R_1 = 0.0416$, $wR_2 = 0.0958$ (all data); Flack parameter −0.03(4).

4.4.3. *O*-9-(2,6-Diisopropylphenylcarbamoyl)quininium (1*S*, 3*S*)-(−)-*cis*-3-(2, 2-dichlorovinyl)-2,2-dimethylcyclopropanecarboxylate 3. $C_{41}H_{51}Cl_2N_3O_5$, $M_r = 736.75$, monoclinic, space group $P2_1$ (no. 4), $a = 9.5029(4)$, $b = 15.3140(6)$, $c = 13.7955(6)$ Å, $\beta = 100.704(2)°$, $V = 1972.69(14)$ $Å^3$, $Z = 2$, $\rho_{calcd} = 1.240$ g cm^{-3}, $\mu = 0.211$ mm^{-1}. Of 172,274 reflections collected up to $\theta_{max} = 28.5°$, 9962 were independent, $R_{int} = 0.0382$, and 9172 were observed ($I > 2\sigma(I)$); final *R* indices: $R_1 = 0.0354$, $wR_2 = 0.0991$ (all data); Flack parameter −0.01(4).

4.4.4. *O*-9-(2,6-Diisopropylphenylcarbamoyl)quininium (1*S*, 3*R*)-(−)-*trans*-3-(2,2-dichlorovinyl)-2,2-dimethylcyclopropanecarboxylate 4. $C_{41.88}H_{53}Cl_2N_3O_5$, $M_r = 749.27$, monoclinic, space group $C2$ (no. 5), $a = 38.3899(19)$, $b = 15.0305(7)$, $c = 9.3888(4)$ Å, $\beta = 96.372(5)°$, $V = 5384.1(4)$ $Å^3$, $Z = 4$, $\rho_{calcd} = 0.924$ g cm^{-3}, $\mu = 0.155$ mm^{-1}. Of 107,372 reflections collected up to $\theta_{max} = 25°$, 4912 were independent, $R_{int} = 0.0739$, and 4912 were observed ($I > 2\sigma(I)$); final *R* indices: $R_1 = 0.0984$, $wR_2 = 0.3161$ (all data).

4.5. Computational details

Single point density-functional theory (DFT) computations were performed on the minima of the complexes obtained at the Hartree–Fock (HF) level of theory using the GAUSSIAN03 program package.[56] Thus, the X-ray structures of the DIPPCQN complexes with DCCA stereoisomers were used as starting geometries for structure optimization at the HF level using a 6-31G(d,p) basis set. The single point energies were then recomputed at the B3LYP[41] density-functional level using Duning's correlation consistent basis set of triple-zeta quality (cc-pvTZ). The energies were finally corrected for basis set superposition errors using counterpoise algorithm.[42]

4.6. ^{1}H NMR experiments

The HCl salt of DIPPCQN was prepared as described previously[24] by adding an excess of HCl (methanolic solution) to the DIPPCQN base, evaporating the solvent and drying in vacuo, which yielded the bis-hydrochloride salt. Then an equimolar amount of DIPPCQN base dissolved in MeOH was added. After the evaporation of the solvent and drying in vacuo, the mono-HCl salt of DIPPCQN was yielded. TEA salts of DCCA were obtained by the addition of stoichiometric amount of TEA to methanolic DCCA stereoisomer solutions, evaporating the solvent and drying in vacuo. 1:1 complexes of DIPPCQN and the individual stereoisomers of DCCA were prepared by dissolving equimolar amounts of the corresponding binding partners.

The signal assignment of ^{1}H NMR spectra of the free DIPPCQN, free *cis*- and *trans*-DCCA, the mono-HCl salt of DIPPCQN, TEA salts of DCCA stereoisomers, and the four individual diastereomeric complexes, viz. DIPPCQN·(1*R*,3*R*)-*cis*-DCCA, DIPPCQN·(1*R*,3*S*)-*trans*-DCCA, DIPPCQN·(1*S*,3*S*)-*cis*-DCCA, DIPPCQN·(1*S*,3*R*)-*trans*-DCCA (1:1 mixtures), was achieved by ^{1}H–{^{1}H} COSY and NOESY.

All spectra were recorded in ACN-D_3 (Aldrich, Vienna, Austria) and in ACN-D_3 containing 0.25% D_3-AcOD (Aldrich) in a diluted solution with a sample concentration of 20 mM. Chemical shifts are given in parts per million (δ) with respect to tetramethyl silane as the standard. The temperature was kept at 25 ± 0.1 °C.

4.7. Additional information

Additional figures illustrating the overlaid diastereomeric X-ray structures from different perspectives, absolute energies of the diastereomeric complexes, comparisons of DFT-optimized geometries with X-ray structures of the four diastereomeric complexes, thermodynamic parameters of adsorption, and complete listings of ^{1}H NMR chemical shifts are available free of charge from the authors.

Acknowledgments

The financial support by the Austrian Christian Doppler Research Society and the industry partners, Merck KGaA (Darmstadt, Germany), AstraZeneca (Mölndal, Sweden), and Fresenius Kabi Austria (Graz, Austria) is gratefully acknowledged. We are indebted to Mr. Alexander Roller for technical assistance with the X-ray diffraction measurements.

References

1. Easson, L. H.; Stedman, E. *Biochem. J.* **1933**, *27*, 1257–1266.
2. Dalgliesh, C. E. *J. Chem. Soc.* **1952**, *137*, 3940–3952.
3. Davankov, V. A. *Chirality* **1997**, *9*, 99–102.
4. Berthod, A. *Anal. Chem.* **2006**, *78*, 2093–2099.
5. Bentley, R. *Arch. Biochem. Biophys.* **2003**, *414*, 1–12.
6. Booth, T. D.; Wahnon, D.; Wainer, I. W. *Chirality* **1997**, *9*, 96–98.
7. Pirkle, W. H. *Chirality* **1997**, *9*, 103.
8. Mesecar, A. D.; Koshland, D. E. *Nature* **2000**, *403*, 614–615.
9. Topiol, S.; Sabio, M. *J. Am. Chem. Soc.* **1989**, *111*, 4109–4110.
10. Garten, S.; Biedermann, U. P.; Agranat, I.; Topiol, S. *Chirality* **2005**, *17*, S159–S170.
11. Petitpas, I.; Bhattacharya, A. A.; Twine, S.; East, M.; Curry, S. *J. Biol. Chem.* **2001**, *276*, 22804–22809.
12. Stahlberg, J.; Henriksson, H.; Divne, C.; Isaksson, R.; Pettersson, G.; Johansson, G.; Jones, T. A. *J. Mol. Biol.* **2001**, *305*, 79–93.
13. Reeder, J.; Castro, P. P.; Knobler, C. B.; Martinborough, E.; Owens, L.; Diederich, F. *J. Org. Chem.* **1994**, *59*, 3151–3160.
14. Kim, S. G.; Kim, K. H.; Jung, J.; Shin, S. K.; Ahn, K. H. *J. Am. Chem. Soc.* **2002**, *124*, 591–596.
15. Kim, S. G.; Kim, K. H.; Kim, Y. K.; Shin, S. K.; Ahn, K. H. *J. Am. Chem. Soc.* **2003**, *125*, 13819–13824.
16. Nagata, H.; Nishi, H.; Kamigauchi, M.; Ishida, T. *Org. Biomol. Chem.* **2004**, *2*, 3470–3475.
17. Li, Z. B.; Lin, J.; Zhang, H. C.; Sabat, M.; Hyacinth, M.; Pu, L. *J. Org. Chem.* **2004**, *69*, 6284–6293.
18. Pirkle, W. H.; Burke, J. A.; Wilson, S. R. *J. Am. Chem. Soc.* **1989**, *111*, 9222–9223.
19. Daeppen, R.; Rihs, G.; Mayer, C. W. *Chirality* **1990**, *2*, 185–189.
20. Pirkle, W. H.; Murray, P. G.; Wilson, S. R. *J. Org. Chem.* **1996**, *61*, 4775–4777.
21. Maier, N. M.; Nicoletti, L.; Lämmerhofer, M.; Lindner, W. *Chirality* **1999**, *11*, 522–528.
22. Machida, Y.; Nishi, H.; Nakamura, K. *Chirality* **1999**, *11*, 173–178.
23. Chankvetadze, B.; Burjanadze, N.; Pintore, G.; Bergenthal, D.; Bergander, K.; Muhlenbrock, C.; Breitkreuz, J.; Blaschke, G. *J. Chromatogr., A* **2000**, *875*, 471–484.
24. Maier, N. M.; Schefzick, S.; Lombardo, G. M.; Feliz, M.; Rissanen, K.; Lindner, W.; Lipkowitz, K. B. *J. Am. Chem. Soc.* **2002**, *124*, 8611–8629.
25. Czerwenka, C.; Lämmerhofer, M.; Maier, N. M.; Rissanen, K.; Lindner, W. *Anal. Chem.* **2002**, *74*, 5658–5666.
26. Czerwenka, C.; Zhang, M. M.; Kaehlig, H.; Maier, N. M.; Lipkowitz, K. B.; Lindner, W. *J. Org. Chem.* **2003**, *68*, 8315–8327.
27. Akasaka, K.; Gyimesi-Forras, K.; Lämmerhofer, M.; Fujita, T.; Watanabe, M.; Harada, N.; Lindner, W. *Chirality* **2005**, *17*, 544–555.
28. Koscho, M. E.; Spence, P. L.; Pirkle, W. H. *Tetrahedron: Asymmetry* **2005**, *16*, 3147–3153.
29. Bicker, W.; Lämmerhofer, M.; Lindner, W. *J. Chromatogr., A* **2004**, *1035*, 37–46.
30. Bicker, W.; Lämmerhofer, M.; Lindner, W., in preparation.
31. Dijkstra, G. D.; Kellogg, R. M.; Wynberg, H.; Svendsen, J. S.; Marko, I.; Sharpless, K. B. *J. Am. Chem. Soc.* **1989**, *111*, 8070–8076.
32. Caner, H.; Biedermann, P. U.; Agranat, I. *Chirality* **2003**, *15*, 637–645.
33. Steiner, T. *Angew. Chem., Int. Ed.* **2002**, *41*, 48–76.
34. Geffrey, G. A.; Saenger, W. *Hydrogen Bonding in Biological Structures*; Springer: Berlin, 1991.
35. Bürgi, T.; Baiker, A. *J. Am. Chem. Soc.* **1998**, *120*, 12920–12926.
36. Wirz, R.; Buergi, T.; Lindner, W.; Baiker, A. *Anal. Chem.* **2004**, *76*, 5319–5330.
37. Lipkowitz, K. B. *J. Chromatogr., A* **2001**, *906*, 417–442.
38. Del Rio, A.; Hayes, J. M.; Stein, M.; Piras, P.; Roussel, C. *Chirality* **2004**, *16*, S1–S11.

39. Götmar, G.; Fornstedt, T.; Guiochon, G. *Chirality* **2000**, *12*, 558–564.
40. DeTar, D. F. *J. Am. Chem. Soc.* **1981**, *103*, 107–110.
41. Lee, A.; Yang, W.; Parr, R. G. *Chem. Phys. Lett.* **1989**, *157*, 200.
42. Van Duijneveldt, F. B.; Van Duijneveldt-Van De Rijdt, J. G. C. M.; Van Lenthe, J. H. *Chem. Rev.* **1994**, *94*, 1873–1885.
43. Oberleitner, W. R.; Maier, N. M.; Lindner, W. *J. Chromatogr., A* **2002**, *960*, 97–108.
44. Asnin, L.; Guiochon, G. *J. Chromatogr., A* **2005**, *1091*, 11–20.
45. Götmar, G.; Asnin, L.; Guiochon, G. *J. Chromatogr., A* **2004**, *1059*, 43–52.
46. Asnin, L.; Kaczmarski, K.; Felinger, A.; Gritti, F.; Guiochon, G. *J. Chromatogr., A* **2006**, *1101*, 158–170.
47. Ajay, W.; Murcko, M. A. *J. Med. Chem.* **1995**, *38*, 4953–4967.
48. Williams, D. H.; Stephens, E.; O'Brien, D. P.; Zhou, M. *Angew. Chem., Int. Ed.* **2004**, *43*, 6596–6616.
49. Lindner, W.; Lämmerhofer, M.; Maier, N. WO 9746557, 1997.
50. *Bruker Programs* SAINT-NT*, version 7.12A;* SADABS*, version 2.10;* XPREP*, version 5.1*; Bruker AXS: Madison, WI, USA, 2003.
51. Sheldrick, G. M. SHELXS*97: Program for Crystal Structure Solution*; University of Göttingen: Germany, 1997.
52. Sheldrick, G. M. SHELXL*97: Program for Crystal Structure Refinement*; University of Göttingen: Germany, 1997.
53. Keller, E. SCHAKAL-*97*; Kristallographisches Institut, University of Freiburg: Germany, 1997.
54. *International Tables for X-ray Crystallography, Volume C, Tables 4.2.6.8 and 6.1.1.4*; Kluwer Academic Press: Dodrecht, The Netherlands, 1992.
55. Crystallographic data (excluding structure factors) for the structures in this paper have been deposited with the Cambridge Crystallographic Data Centre as Supplementary Publication Numbers CCDC 665833–665836. Copies of the data can be obtained, free of charge, on application to CCDC, 12 Union Road, Cambridge CB2 1EZ, UK [fax: +44(0)-1223-336033 or e-mail: deposit@ccdc.cam.ac.uk].
56. Frisch, M. J.; Trucks, G. W.; Schlegel, H. B.; Scuseria, G. E.; Robb, M. A.; Cheeseman, J. R.; Montgomery, J. A.; Vreven, T.; Kudin, K. N.; Burant, J. C.; Millam, J. M.; Iyengar, S. S.; Tomasi, J.; Barone, V.; Mennucci, B.; Cossi, M.; Scalmani, G.; Rega, N.; Petersson, G. A.; Nakatsuji, H.; Hada, M.; Ehara, M.; Toyota, K.; Fukuda, R.; Hasegawa, J.; Ishida, M.; Nakajima, T.; Honda, Y.; Kitao, O.; Nakai, H.; Klene, M.; Li, X.; Knox, J. E.; Hratchian, H. P.; Cross, J. B.; Bakken, V.; Adamo, C.; Jaramillo, J.; Gomperts, R.; Stratmann, R. E.; Yazyev, O.; Austin, A. J.; Cammi, R.; Pomelli, C.; Ochterski, J. W.; Ayala, P. Y.; Morokuma, K.; Voth, G. A.; Salvador, P.; Dannenberg, J. J.; Zakrzewski, V. G.; Dapprich, S.; Daniels, A. D.; Strain, M. C.; Farkas, O.; Malick, D. K.; Rabuck, A. D.; Raghavachari, K.; Foresman, J. B.; Ortiz, J. V.; Cui, Q.; Baboul, A. G.; Clifford, S.; Cioslowski, J.; Stefanov, B. B.; Liu, G.; Liashenko, A.; Piskorz, P.; Komaromi, I.; Martin, R. L.; Fox, D. J.; Keith, T.; Al-Laham, M. A.; Peng, C. Y.; Nanayakkara, A.; Challacombe, M.; Gill, P. M. W.; Johnson, B.; Chen, W.; Wong, M. W.; Gonzalez, C.; Pople, J. A. GAUSSIAN *03, Revision D.01*; Gaussian: Wallingford, CT, 2004.